

Influence of Nuclear Quadrupole Moments on Electron Spin Coherence in Semiconductor Quantum Dots

Erik Welander,¹ Evgeny Chekhovich,² Alexander Tartakovskii,² and Guido Burkard¹

¹*Department of Physics, University of Konstanz, Germany*

²*Department of Physics and Astronomy, University of Sheffield, United Kingdom*

We theoretically investigate the influence of the fluctuating Overhauser field on the spin of an electron confined to a quantum dot (QD). The fluctuations arise from nuclear angular momentum being exchanged between different nuclei via the nuclear magnetic dipole coupling. We focus on the role of the nuclear electric quadrupole moments (QPMs), which generally cause a reduction in inter-nuclear spin transfer efficiency in the presence of electric field gradients. The effects on the electron spin coherence time are studied by modeling an electron spin echo experiment. We find that the QPMs cause an increase in the electron spin coherence time and that an inhomogeneous distribution of the quadrupolar shift, where different nuclei have different shifts in energy, causes an even larger increase in the electron coherence time than a homogeneous distribution. Furthermore, a partial polarization of the nuclear spin ensemble amplifies the effect of the inhomogeneous quadrupolar shifts, causing an additional increase in electron coherence time, and provides an alternative to the experimentally challenging suggestion of full dynamic nuclear spin polarization.

PACS numbers: 71.70.Jp, 73.21.La, 76.60.Lz, 74.25.nj

I. INTRODUCTION

Using the spin of an electron confined to a quantum dot (QD) has been proposed as one possible implementation of a qubit¹. One of the hardest challenges of its practical realization is the fast decoherence of the electron spin caused by its interaction with the effective, time-varying magnetic field known as the Overhauser field²⁻⁹. Physically, the Overhauser field originates from the hyperfine interaction between the electron spin and nuclear spins of the QD. The exchange of spin between different nuclei via dipolar coupling combined with an inhomogeneous hyperfine coupling strength lead to a time-varying Overhauser field. The loss of electron spin coherence can be partially avoided by applying a π -pulse at time $t = T/2$ causing a reversal of the electron spin propagation and leading to an electron spin echo at time $t = T$ ¹⁰⁻¹². However, if the Overhauser field varies in the interval $[0, T]$, the electron spin state cannot be fully restored. Techniques to prolong the electron coherence time by reducing the fluctuations of the nuclear spins have been theoretically suggested¹³⁻²² and experimentally tested^{6,23-31}. In this paper, we study the effects of nuclear quadrupolar shifts which impede the transfer of nuclear spin by causing certain transitions to be energetically forbidden.

An atomic nucleus having a non-uniform charge distribution may possess an electric quadrupole moment^{11,12,32} which couples to electric field gradients (EFGs) causing a shift in energy, known as the quadrupolar shift. The EFGs can be external, originate from neighboring atoms not participating in the nuclear spin transfer processes, or due to strain. We focus on the special case for which the EFGs have in-plane symmetry and where the symmetry axis coincides with the axis of an externally applied magnetic field, $\mathbf{B} = B_0 \hat{z}$. This leads to a quadrupolar shift in energy proportional to $I_z^2 + c$, where $\mathbf{I} = (I_x, I_y, I_z)^T$

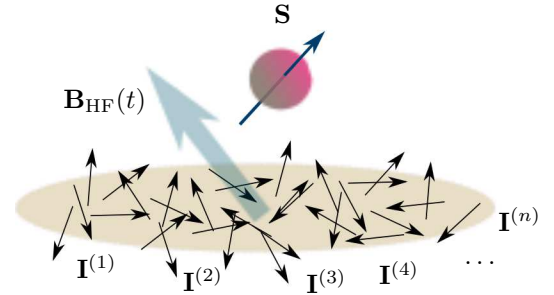


Figure 1. Illustration of the QD containing many nuclear spins (black arrows) each with corresponding operator $\mathbf{I}^{(n)}$. The nuclear spins couple to an electron spin (red ball with arrow) via the hyperfine Hamiltonian and give rise to an effective magnetic field (large blue arrow). Because of the transfer of nuclear spin between different nuclei and the inhomogeneous hyperfine coupling strength, the effective magnetic field is fluctuating in time and is given by the stochastic vector $\mathbf{B}_{HF}(t)$.

is the nuclear spin operator and c is a constant.

Recent experimental work³⁵ shows a significant increase in nuclear coherence times when quadrupolar energy shifts were introduced via strain. This suggests that the nuclear QPMs could be used as a way to prolong electron coherence times and provides an alternative to the experimentally challenging technique of complete dynamic nuclear spin polarization. In this paper, we try to estimate the effect of the nuclear QPMs on the electron spin coherence and its limitations.

In QDs, EFGs are primarily caused by strain^{11,26,36-40}, leading to displacements of the nuclei which in turn cause a modification of the charge distribution. If the nuclear displacement varies slowly over the QD and the QPMs are to a good approximation equal for all nuclei, the quadrupolar shift is homogenous and may be modeled

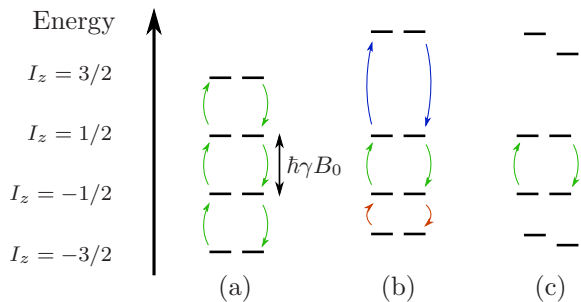


Figure 2. Energy level scheme of two nuclear spins $I = 3/2$ under the influence of an external magnetic field B_0 along \hat{z} and quadrupolar shifts. The external magnetic field causes a Zeeman splitting of $\hbar\gamma B_0$ between spin levels differing by $\Delta I_z = 1$. (a) Without any quadrupolar shifts, any two neighboring energy levels differ by the same energy, thus allowing any transition for which the total nuclear spin along \mathbf{B} is conserved. (b) With homogeneous quadrupolar shifts, all energy levels are shifted by an amount proportional to I_z^2 and transitions with different sets of initial and final states are inhibited. (c) With inhomogeneous quadrupolar shifts the energy levels of different nuclei are shifted by different amounts and only the $-1/2 \leftrightarrow 1/2$ transitions are energetically allowed. Here we have omitted any constant shift in energy, i.e. not depending on I_z , since it does not contribute to the nuclear spin dynamics.

by an additional term in the Hamiltonian which is equal for all nuclei. This may be the case when external strain is applied. If the stress is caused by a lattice mismatch at the interface between different materials (e.g. GaAs and InAs), the change in charge distribution will be more random, causing an inhomogeneous quadrupolar shift that differs between different nuclear spins. In addition, the random location of dopants is another source of inhomogeneous quadrupolar shifts³⁵.

II. THEORETICAL MODEL

We study the dynamics of a single electron spin in a QD, containing N atomic nuclei, each having spin I in the presence of an external magnetic field, \mathbf{B} . The electron and nuclear spins are influenced by each other via the hyperfine coupling, which we model with the Hamiltonian

$$H_{\text{HF}} = \mathbf{S} \cdot \sum_{n=1}^N A_n \mathbf{I}^{(n)}, \quad (1)$$

where n enumerates the atomic sites, A_n are hyperfine coupling strengths^{5,7}, \mathbf{S} is the electron spin operator and $\mathbf{I}^{(n)}$ are the nuclear spin operators. The hyperfine coupling strengths depend on the atomic species and are proportional to $|\Psi(\mathbf{r}_n)|^2$ where $\Psi(\mathbf{r}_n)$ is the electron envelope function at the atom site n with the position \mathbf{r}_n . The nuclei are mutually coupled by their magnetic dipole

moments¹¹ as described by the Hamiltonian

$$H_{\text{D}} = \sum_{n < m} \alpha_{nm} \left(\frac{\mathbf{I}^{(n)} \cdot \mathbf{I}^{(m)}}{r_{nm}^3} - 3 \frac{[\mathbf{I}^{(n)} \cdot \mathbf{r}_{nm}][\mathbf{I}^{(m)} \cdot \mathbf{r}_{nm}]}{r_{nm}^5} \right), \quad (2)$$

where $\alpha_{nm} = \gamma_n \gamma_m \hbar^2 \mu_0 / 4\pi$ with the nuclear gyromagnetic ratios γ_n , $\mathbf{r}_{nm} = \mathbf{r}_n - \mathbf{r}_m$, and $r_{nm} = |\mathbf{r}_{nm}|$. In the presence of a strong magnetic field, the terms of Eq. (2) not preserving the total nuclear spin projection along \mathbf{B} are strongly suppressed. Assuming $\mathbf{B} = B_0 \hat{z}$ we can make the secular approximation

$$H_{\text{D}'} = \sum_{n < m} \alpha'_{nm} \left[I_z^{(n)} I_z^{(m)} - \frac{1}{4} (I_+^{(n)} I_-^{(m)} + I_-^{(n)} I_+^{(m)}) \right], \quad (3)$$

where $\alpha'_{nm} = \gamma_n \gamma_m \hbar^2 (1 - \cos^2 \theta_{nm}) / r_{nm}^3$ and θ_{nm} is the angle between \mathbf{r}_{nm} and \hat{z} . The nuclear spins are further influenced by the electric quadrupole moments which, for the special case of planar symmetry and when the quadrupolar symmetry axis coincides with \hat{z} , can be modeled by the Hamiltonian

$$H_{\text{Q}} = h \sum_n \nu_Q^{(n)} I_z^{(n)2}, \quad (4)$$

where we choose not to include any constant shift in energy since it would not affect the nuclear spin dynamics. In principle this model could be used for several nuclear species at once, such as ⁶⁹Ga, ⁷¹Ga, and ⁷⁵As. However, different species typically have different gyromagnetic ratios and consequently have different spin transition energies. For this reason, the spin transfer between different nuclear species at high magnetic fields is strongly suppressed, and we include only one nuclear species.

The quantum state of the whole quantum dot including nuclear and electron spins is an element of the product Hilbert space $\mathcal{H} = \mathcal{H}_N \otimes \mathcal{H}_e$, where $\mathcal{H}_N = \mathcal{H}_I^{\otimes N}$ is the Hilbert space of the nuclear spins, \mathcal{H}_I is the Hilbert space of one nuclear spin which is spanned by $\{|-I\rangle, |-I+1\rangle, \dots, |I-1\rangle, |I\rangle\}$, and \mathcal{H}_e is the Hilbert space of the electron spin spanned by $\{|\uparrow\rangle, |\downarrow\rangle\}$. In principle, the time evolution of any initial state $|t=0\rangle \in \mathcal{H}$ is given by $|t>0\rangle = e^{-iHt/\hbar} |t=0\rangle$ from the solution to the Schrödinger equation, where

$$H = H_{\text{D}'} + H_{\text{Q}} + H_{\text{HF}} + H_{\text{Z}} \quad (5)$$

and

$$H_{\text{Z}} = \hbar \mathbf{B} \cdot \left(\gamma_e \mathbf{S} + \gamma \sum_n \mathbf{I}^{(n)} \right) \quad (6)$$

is the combined electron and nuclear Zeeman term with the electron gyromagnetic ratio $\gamma_e = g_e \mu_B / \hbar$, where g_e is the electron g -factor and μ_B is the Bohr magneton. However, the dimension of the Hilbert space, $\dim \mathcal{H} = 2(2I+1)^N$, grows exponentially with the number of nuclear spins N , and for a typical quantum dot

containing 10^4 to 10^6 nuclei, a direct numerical calculation of its time evolution is unrealistic. To make a suitable approximation, we divide the problem into two parts by decoupling the electron from the nuclear spins. This allows us to consider a sample of fewer nuclear spins for which the spin dynamics are first simulated and then used as an input to the electronic problem.

To study the nuclear spin dynamics we consider a set of $M \ll N$ nuclei. From the eigenstates of $I_z^{(n)}$ for each nuclear spin we construct initial product states $|\mathbf{m}_0, t=0\rangle = |\mathbf{m}_0\rangle \in \mathcal{H}_M$, where $|\mathbf{m}\rangle = |m_z^{(1)}, m_z^{(2)} \dots m_z^{(M)}\rangle = |m_z^{(1)}\rangle \otimes |m_z^{(2)}\rangle \otimes \dots \otimes |m_z^{(M)}\rangle$ and $m_z^{(n)}$ is the projection of the n -th nuclear spin along \hat{z} . The product states are eigenstates of the total nuclear spin projection operator along \hat{z} , $I_z = \sum_{n=1}^M I_z^{(n)}$ with eigenvalues $\sum_{n=1}^M m_z^{(n)}$, and are evolved directly by $|\mathbf{m}_0, t > 0\rangle = e^{-iH't/\hbar} |\mathbf{m}_0\rangle$, where $H' = H_{D'} + H_Q$ is the Hamiltonian of the nuclear spins. The time-evolved state vector gives the probability function for the eigenstates $|\mathbf{m}\rangle$ of I_z as $p_{\mathbf{m}_0}(\mathbf{m}, t) = \langle \mathbf{m} | \mathbf{m}_0, t \rangle^2$ and from this probability function we define a stochastic vector $\mathbf{m}(t) = (m_z^{(1)}, m_z^{(2)} \dots m_z^{(n)})$ with probability $p_{\mathbf{m}_0}(\mathbf{m}, t)$. The effective magnetic field from any product state $|\mathbf{m}\rangle$ is given by

$$\mathbf{B}_{\text{HF}}(\mathbf{m}) = B(\mathbf{m})\hat{z} \quad (7)$$

where

$$B(\mathbf{m}) = \left\langle \mathbf{m} \left| \sum_{n=1}^M A_n \mathbf{I}^{(n)} \right| \mathbf{m} \right\rangle = \sum_{n=1}^M A_n m_z^{(n)}. \quad (8)$$

The hyperfine field \mathbf{B}_{HF} has vanishing components along \hat{x} or \hat{y} since $\langle \mathbf{m} | I_x^{(n)} | \mathbf{m} \rangle = \langle \mathbf{m} | I_y^{(n)} | \mathbf{m} \rangle = 0$ for any \mathbf{m} and n . Using the previously defined stochastic $\mathbf{m}(t)$, we obtain a discrete-valued stochastic magnetic field

$$B(t) = B(\mathbf{m}(t)) \quad (9)$$

with non-Markovian dynamics. Although the probability function of $p_{\mathbf{m}_0}(\mathbf{m}, t)$ is given by the time evolution for any \mathbf{m}_0 , $B(t)$ is still a stochastic variable.

For a given $B(t)$, finding the electron spin dynamics is straight-forward by considering the Hamiltonian

$$H_e(t) = S_z(B(t) + \hbar\gamma_e B_0), \quad (10)$$

which describes the time-evolution of an initial state by $|t > 0\rangle = e^{-i \int_0^t H_e(t') dt'/\hbar} |t = 0\rangle$. The effects of the static magnetic field B_0 is completely cancelled by the electron spin echo and hence this term may be excluded from the dynamics. Formally this can be achieved by going over to the rotating frame^{11,12}.

In order to study the electron spin echo we let the electron spin state be given by $|t\rangle = c_\uparrow(t)|\uparrow\rangle + c_\downarrow(t)|\downarrow\rangle$ and choose $c_\uparrow(0) = c_\downarrow(0) = 1/\sqrt{2}$. $H_e(t)$ is diagonal in

the eigenbasis of S_z and the time evolution is directly given by

$$|t\rangle = \frac{e^{-i\varphi(t)}|\uparrow\rangle + e^{i\varphi(t)}|\downarrow\rangle}{\sqrt{2}}, \quad (11)$$

where $\varphi(t) = \int_0^t B(t') dt'/2$ and since we are using the rotating frame there is no extra phase difference from the electron Zeeman splitting. The change in electron spin state due to the evolving $\varphi(t)$ can be partially undone by applying a π -pulse around \hat{x} at $t = T/2$ which transforms the electron state according to $\alpha|\uparrow\rangle + \beta|\downarrow\rangle \rightarrow \beta|\uparrow\rangle + \alpha|\downarrow\rangle$ and at time $t = T$ the electron spin will be in the state $|T\rangle = (e^{2i\varphi(T/2)-i\varphi(T)}|\uparrow\rangle + e^{-2i\varphi(T/2)+i\varphi(T)}|\downarrow\rangle)/\sqrt{2}$. We denote the projection onto the initial electron state by

$$\lambda[B(t)](T) = \langle T|0\rangle = \cos[2\varphi(T/2) - \varphi(T)], \quad (12)$$

which gives a measure of the quality of the electron echo as a function of echo time. An exhaustive description of the electron dynamics from a given initial nuclear state $|\mathbf{m}_0\rangle$ is given by averaging over all possible temporal realizations

$$f_{\mathbf{m}_0}(T) = \int \lambda[B(t)](T) p_{\mathbf{m}_0}[B(t)][DB(t)], \quad (13)$$

where $p_{\mathbf{m}_0}[B(t)]$ is the probability density functional taking a function $B(t)$ as a parameter³³, and the $\int \dots [DB(t)]$ denotes the functional integration over all possible $B(t)$. However, except for the case of the fully polarized initial state when $\mathbf{m}_0 = \pm(I, I, \dots, I)$, the set of all possible temporal realizations is infinite and since the $p(B(t), t)$ needs to be calculated numerically, $f_{\mathbf{m}_0}(T)$ is approximated by performing a set of random walks instead. For this purpose we let $B(t) = \sum_{n=1}^M A_n m_z^{(n)}(t)$ be given for a discrete set of times by randomly selecting $\mathbf{m}(t)$ with probabilities $p_{\mathbf{m}_0}(\mathbf{m}, t)$. This way we obtain the approximation

$$\tilde{f}_{\mathbf{m}_0}(T) = \frac{1}{K} \sum_{k=1}^K \lambda[B_k(t)](T), \quad (14)$$

and K is the number of samples and $B_k(t)$ are the randomly chosen realizations of the Overhauser field. This differs from a typical random walk of Monte-Carlo type since the steps are chosen from a time dependent probability distribution leading to non-Markovian dynamics.

A typical electron spin echo experiment consists of averaging several measurements for which the initial nuclear states do not need to be identical. To incorporate this we define an average fidelity for a set of L measurements according to

$$F(T) = \frac{1}{L} \left(\sum_{l=1}^L \tilde{f}_{\mathbf{m}_l}(T) \right)^2, \quad (15)$$

where \mathbf{m}_i represent the initial nuclear states, from which the probability distribution $p_{\mathbf{m}_i}(\mathbf{m}, t)$ is calculated numerically. The initial states are in turn chosen randomly with the thermal equilibrium probabilities

$$p(\mathbf{m}) = \frac{1}{Z} \exp \left[-\frac{\hbar\gamma B_0 \sum_n m_z^{(n)}}{k_B T_N} \right], \quad (16)$$

where we have used the partition sum

$$Z = \sum_{\mathbf{m}} \exp \left[-\frac{\hbar\gamma B_0 \sum_n m_z^{(n)}}{k_B T_N} \right], \quad (17)$$

and where T_N is the nuclear spin temperature. We define the nuclear spin polarization as $\eta = -\langle I_z \rangle / NI$ with $\langle I_z \rangle = \sum_{\mathbf{m}} p(\mathbf{m}) \sum_{n=1}^N m_z^{(n)}$ which leads to the relation

$$\eta = \tanh \frac{g_N \mu_0 B_0}{2k_B T_N} \quad (18)$$

between η and B_0/T_N .

III. RESULTS

Using ensembles of 6 spins $I = 3/2$, arranged on a line with $\mathbf{r}_n = an\hat{x}$ for $n = 1 \dots 6$ and $a = 5.56 \text{ \AA}$, for each parameter set of polarization and quadrupolar shifts we performed $K = 10000$ random walks for each of $L = 1000$ random initial states producing typical fidelity vs. echo time curves shown in Fig. 3. We used the hyperfine couplings $A_n = Ae^{-n^2/6^2}$ to model the varying coupling strength for an electron in a QD. A was adjusted to give a typical³⁴ electron spin coherence time of 1 ms for the unpolarized case and without quadrupolar shifts. Rather than in the absolute coherence time, we are primarily interested in the change of the coherence time due to polarization and quadrupolar shifts. Experiments^{35,37-41} report QP shifts up to several MHz, and in initial calculations we investigated QP shifts in the MHz range. However, we found that the electron spin coherence does not change significantly when exceeding 2 kHz, and thus we limit the quadrupolar shifts to 2 kHz in our calculations. In order to systematically study the effects of polarization and quadrupole moments, we fit the echo curve to the function

$$f(T) = (1 - F_\infty) \exp(-T^4/T_2^4) + F_\infty, \quad (19)$$

where T_2 will be called the coherence time and F_∞ is an asymptotic value. Physically, the two terms can be regarded as the nuclear spin ensemble having both a fluctuating part causing the decaying term and a static one giving rise to the asymptote F_∞ . The form of the exponential T^4 decay can be found by considering low-frequency noise⁴².

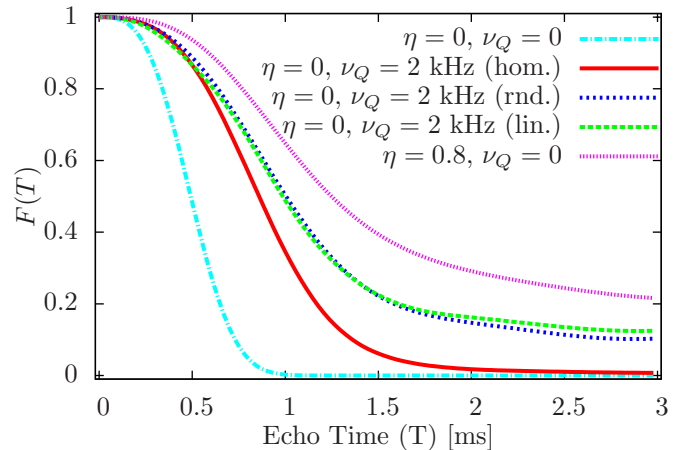


Figure 3. Typical electron spin echo curves for various nuclear parameters. The cyan line shows the electron spin echo without quadrupolar moments and nuclear polarization. The red line shows the effect of including a homogeneous quadrupolar shift of 2 kHz. The blue and green lines show the effect of 2 kHz random and linear inhomogeneous quadrupolar shift, where the inhomogeneity is characterized by a random distribution and linear gradient respectively, described below. The purple line shows the effect of nuclear spin polarization of 80%. We observe that for a highly polarized nuclear spin ensemble, as for the situation with large inhomogeneous quadrupolar shifts, the echo fidelity does not vanish completely even at long times.

A. Effect of polarization

We begin with studying the effects of increasing the nuclear polarization without including quadrupole moments. Fig. 4 shows the electron spin coherence time T_2 and the asymptotic fidelity F_∞ as a function of nuclear spin polarization η . For increasing nuclear spin polarization both electron spin coherence time and fidelity asymptote increase. The increasing F_∞ suggests that the nuclear spin dynamics is not only slowed down but also that there is a growing part of the nuclear spin ensemble that remains static. For a complete polarization $\eta = 1$ the nuclear spins become completely static and $T_2 \rightarrow \infty$ and/or $F_\infty \rightarrow 1$. This is an expected result and polarizing the nuclear spins has been proposed as a method to prolong electron coherence times. Practically, this method has proven to be challenging and so far $\eta = 65\%$ is the maximal dynamic nuclear spin polarization reported²⁹, which further motivates searching for alternative ways to reduce the nuclear spin fluctuations.

B. Effect of quadrupolar shifts

We now turn our attention to the quadrupole moments. As described in the introduction, there is a significant difference between homogeneous quadrupolar shifts, where

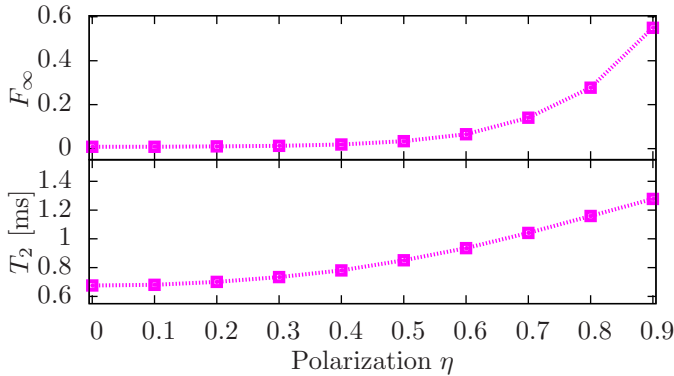


Figure 4. Effect of increased nuclear spin polarization. When the nuclear spin polarization is increased, both electron coherence time T_2 and asymptotic fidelity F_∞ increase. Not shown in the figure is the situation of $\eta = 1$, which would lead to a unit asymptotic fidelity or infinite electron coherence time.

all nuclear spins experience the same shifts in energy, and inhomogeneous quadrupolar shifts, where each nuclear spin may experience a different effect. Using an unpolarized ensemble of $M = 6$ nuclear spins as before, the homogeneous quadrupolar shifts are modeled by

$$H_Q = h\nu_Q \sum_{n=1}^M I_z^{(n)2}. \quad (20)$$

For the inhomogeneous quadrupolar shift we investigate two different distributions and use the Hamiltonian

$$H_Q = \frac{2h\nu_Q}{M-1} \sum_{n=1}^M (n-1) I_z^{(n)2} \quad (21a)$$

$$H_Q = \frac{h\nu_Q}{Y} \sum_{n=1}^M X_n I_z^{(n)2}, \quad (21b)$$

where $X_n \sim U(0,1)$ and $Y = \sum_{n=1}^M X_n/M$, so that the average quadrupolar shift is ν_Q all cases. The Hamiltonian (21a) describes a linear gradient in quadrupolar shifts and Eq. (21b) describes random quadrupolar shifts. Fig. 5 shows the effect of homogeneous and inhomogeneous quadrupolar shifts on the electron coherence time and asymptotic fidelity, which in both cases increases with increasing QP strengths ν_Q . Furthermore, we note that the inhomogeneous quadrupolar shifts lead to marginally longer electron coherence times than the homogeneous ones. Finally we note that there also is a difference in the asymptotic value F_∞ between the homogeneous and inhomogeneous case. For the inhomogeneous QP shifts the asymptotic value increases, an effect that is almost absent for the homogeneous case. There is, however, not a large difference between the linear and random inhomogeneous QP shifts. Comparing to the effect of inhomogeneous quadrupolar moments to the one of increased nuclear polarization without QP shifts shown in Fig. 4, we find similar coherence times and fidelity

asymptote at $\eta = 70\%$ and $\nu_Q = 2$ kHz, suggesting both can be used as a way of increasing electron coherence time. This supports the idea that quadrupole moments may be used to obtain a quantum dot with a frozen nuclear bath, as proposed recently³⁵.

C. Combined effect of polarization and quadrupolar shift

When both inhomogeneous quadrupolar shifts and nuclear spin polarization are included, we expect to see further enhancement of the electron spin echo. For a partial polarization, the population of nuclear spins will be dominated by $I_z = 3/2$ and $I_z = 1/2$ states. On the other hand, inhomogeneous quadrupolar shifts effectively suppress transitions between these states and the nuclear spins should remain mostly static. Fig. 6 shows the echo fidelity $F(T)$ when quadrupolar shifts are introduced to an ensemble of nuclear spins with 70% polarization. For homogeneous QP shifts there is little change in the electron coherence but for inhomogeneous QP shifts, the electron spin coherence is strongly increased to levels above the one corresponding to $\nu_Q = 0$ and a degree of polarization of $\eta = 90\%$, shown in Fig. 5. We also observe that

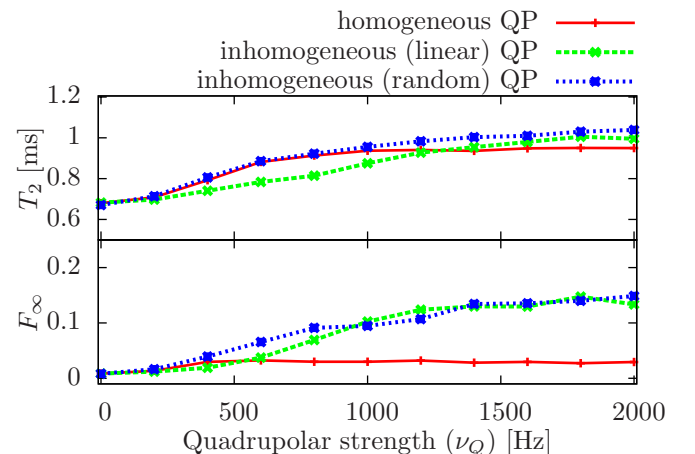


Figure 5. Electron coherence time T_2 and asymptotic fidelity F_∞ including homogeneous (red curves), linear (green curves, Eq. (21b)), and random (blue curves, Eq. (21b)) inhomogeneous QP shifts. *Upper panel:* Electron coherence times T_2 . For high QP strengths, the inhomogeneous shift leads to marginally longer electron coherence times since all transitions except between $I_z = -1/2$ and $I_z = 1/2$ are energetically forbidden. For small QP strengths, the inhomogeneous shift may lead to a smaller change in electronic coherence times than for the homogeneous shift because parts of the nuclear system experience a relatively small shift in transition energy. *Lower panel:* The asymptotic fidelity F_∞ of the electron spin. At higher quadrupolar shifts, the inhomogeneous case resembles the effects of increased nuclear spin polarization. There is almost no difference between the linear and random inhomogeneous shifts but the effect is not observed for homogeneous quadrupolar shift.

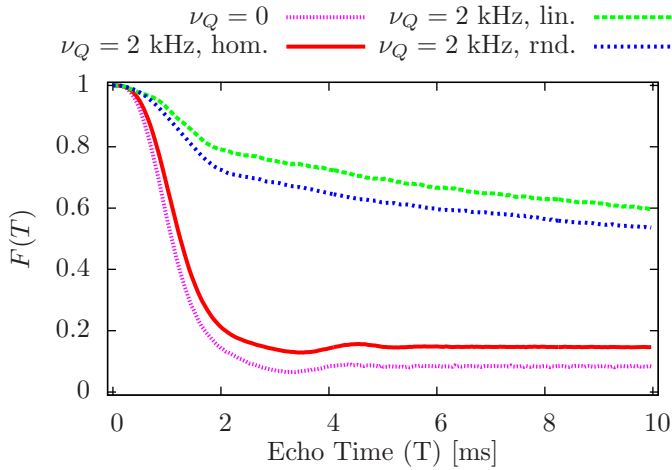


Figure 6. Echo fidelity for a nuclear spin ensemble of polarization $\eta = 0.7$ with linear (green curve) and random (blue) inhomogeneous quadrupolar shifts as well as with homogeneous (red curve) QP shift and without quadrupolar shift (purple curve). The inclusion of inhomogeneous quadrupolar shifts leads to a significant change in the coherence of the electron. There is a clear change in slope around $T = 2$ ms corresponding to the transitions between the two different time scales. The homogeneous quadrupolar shifts do not have a large effect on the electron coherence.

there seems to be two time scales for the decay of the electron spin coherence. For this reason we extend the fitting function to

$$f(T) = F_a e^{-T^4/T_{2a}^4} + F_b e^{-T^4/T_{2b}^4} + F_\infty, \quad (22)$$

where $F_a + F_b + F_\infty = 1$. Here, T_{2a} corresponds to the decoherence of the part of the nuclear ensemble fluctuating rapidly by the unsuppressed $-1/2 \leftrightarrow 1/2$ transitions and T_{2b} corresponds to the slowly fluctuating part exchanging spin via the inhibited transitions. The two coherence times T_{2a} and T_{2b} are shown as functions of the quadrupolar shift in Fig. 7. T_{2b} increases strongly for increasing quadrupolar shift, supporting the claim that this is related to the population undergoing inhibited transitions, while T_{2a} is largely unaffected by the QP shifts which indicates that this is caused by the allowed spin $I_z = 1/2 \leftrightarrow I_z = -1/2$ transitions. The effect on the asymptotic fidelity F_∞ can be seen in Fig. 8. For both linear and random quadrupolar distribution F_∞ increases as a function of ν_Q and reaches values over 50% similar to the ones found for a polarization of $\eta = 90\%$ for the case of $\nu_Q = 0$, shown in Fig. 4. The ratio F_b/F_a shows a weak increase with ν_Q , indicating that the slow decoherence increase in relative magnitude to the fast one. Together, the increasing F_∞ and F_b/F_a demonstrate a simultaneous reduction of decoherence rates and an increase in final coherence. For weak quadrupolar shifts $\nu_Q < 600$ Hz the reduction of nuclear spin transfer is too small for F_b and T_{2b} to be accurately distinguished and determined.

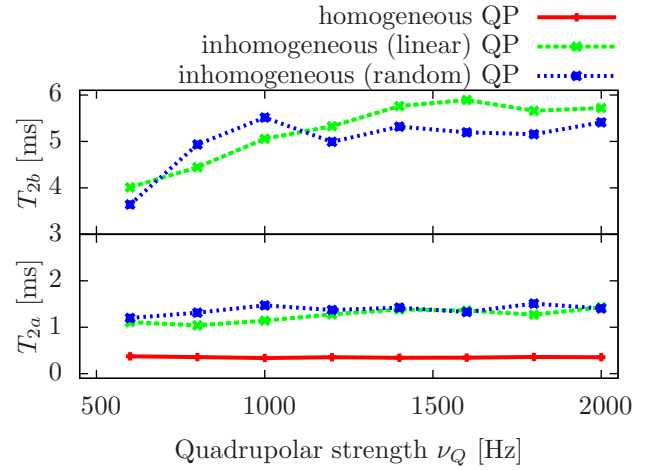


Figure 7. The two coherence times T_{2a} and T_{2b} for homogeneous (red curve), linear inhomogeneous (green curve) and random inhomogeneous (blue curve) quadrupolar shifts including $\eta = 70\%$ nuclear polarization. *Upper panel:* The slow decoherence T_{2b} corresponding to inhibited transitions which strongly increases with increasing quadrupolar strength ν_Q . There is little difference between linear and random inhomogeneous distribution. For the homogeneous QP distribution, there is no observed slow decoherence, and no T_{2b} can be found. *Lower panel:* The fast decoherence T_{2a} corresponding to the $-1/2 \leftrightarrow 1/2$ which remains relatively constant when the quadrupolar strength is increased.

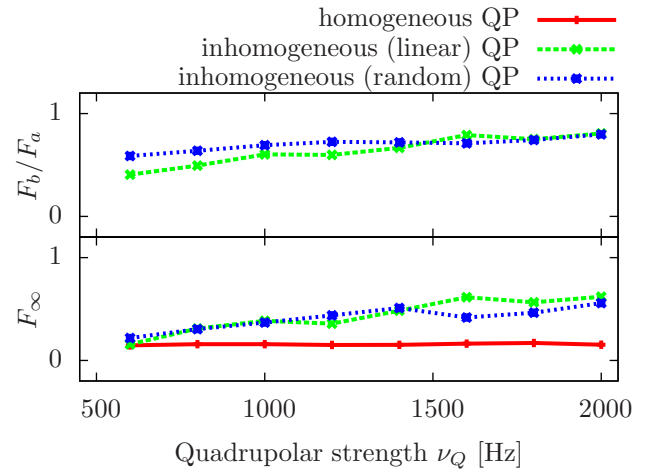


Figure 8. The coherence weights F_a , F_b , and F_∞ for different quadrupolar strengths and distributions when using $\eta = 70\%$ nuclear polarization. *The upper panel* shows the ratio F_b/F_a between slow and fast electron decoherence. For increasing quadrupolar strength, there is a small increase in the slow part, but little difference between linear and random quadrupolar shift distribution. *The lower panel* shows the asymptotic fidelity F_∞ . For both distributions of inhomogeneous quadrupolar shifts, there is a clear increase with increasing quadrupolar strength while the homogeneous distribution remains practically constant.

IV. DISCUSSION AND CONCLUSIONS

We have investigated the effect of nuclear quadrupole moments (QPMs) on the coherence time T_2 of an electron in a quantum dot undergoing an electron spin echo. We found that the presence of QPMs together with electric field gradients increase the electron coherence time. The effect is larger if inhomogeneous quadrupolar shifts are present than in the case of homogeneous shifts. For the inhomogeneous case, the effect on the electron spin coherence is similar to that of increased nuclear spin polarization, suggested as an alternative method to prolong electron coherence. We found almost no difference between the two investigated distributions of quadrupolar shifts (linear and random). The impact of the QPMs is significantly increased if the nuclear spin ensemble is also partially polarized, leading to a greater population

of the nuclear spin states which can only transfer spin via inhibited processes. This suggests applying the existing technique of partially polarizing the nuclear spins dynamically to quantum dots having a large built-in or externally applied inhomogeneous strain, which would lead to a significant increase of electron coherence times not achievable using only dynamic nuclear spin polarization with existing methods. Our findings also support recent suggestions³⁵ to utilize the QPMs to create a quantum dot nearly free from nuclear spin fluctuations.

ACKNOWLEDGMENTS

We acknowledge funding from the Konstanz Center of Applied Photonics (CAP), BMBF under the program QuaHL-Rep and from the European Union through Marie Curie ITN S³NANO. E.A.C. was supported by a University of Sheffield Vice-Chancellor's Fellowship.

-
- ¹ D. Loss and D. P. DiVincenzo, Phys. Rev. A **57**, 120 (1998).
² S. I. Erlingsson *et al.*, Phys. Rev. B **64**, 195306 (2001).
³ I. A. Merkulov *et al.*, Phys. Rev. B **65**, 205309 (2002).
⁴ A. V. Khaetskii *et al.*, Phys. Rev. Lett. **88**, 186802 (2002).
⁵ W. A. Coish and J. Baugh, Phys. Stat. Sol. B **246**, No. 10, 2203-2215 (2009).
⁶ J. R. Petta *et al.*, Science, **309**, 2180 (2005).
⁷ W. A. Coish and D. Loss, Phys. Rev. B **70**, 195340 (2004).
⁸ J. Fischer *et al.*, Sol. Stat. Comm. **149** 1443-1450 (2009).
⁹ H. Kurtze *et al.*, Phys. Rev. B **85**, 195303 (2012).
¹⁰ X. J. Wang *et al.*, Phys. Rev. Lett. **109**, 237601 (2012).
¹¹ C. P. Slichter, *Principles of Magnetic Resonance*, Springer (1990).
¹² A. Abragam, *Principles of Nuclear Magnetism*, Oxford (1961).
¹³ W. Yao *et al.*, Phys. Rev. B **74**, 195301 (2006).
¹⁴ S. E. Economou and E. Barnes, Phys. Rev. B **89**, 165301 (2014).
¹⁵ W. M. Witzel and S. Das Sarma, Phys. Rev. B **74**, 035322 (2006).
¹⁶ W. M. Witzel and S. Das Sarma, Phys. Rev. Lett. **98**, 077601 (2007).
¹⁷ D. Stepanenko *et al.*, Phys. Rev. Lett. **96**, 136401 (2006).
¹⁸ H. Ribeiro and G. Burkard, Phys. Rev. Lett. **102**, 216802 (2009).
¹⁹ B. Lee *et al.*, Phys. Rev. Lett. **100**, 160505 (2008).
²⁰ K. Khodjasteh and D. A. Lidar, Phys. Rev. A **75**, 062310 (2007).
²¹ G. S. Uhrig, Phys. Rev. Lett. **98**, 100504 (2007).
²² S. Takahashi *et al.*, Phys. Rev. Lett. **101**, 047601 (2008).
²³ C. Kloeffel *et al.*, Phys. Rev. Lett. **106**, 046802 (2011).
²⁴ H. Bluhm *et al.*, Nat. Phys. **7**, 113 (2010).
²⁵ H. Bluhm *et al.*, Phys. Rev. Lett. **105**, 216803 (2010).
²⁶ R. I. Dzhioev and V. L. Korenev, Phys. Rev. Lett. **99**, 037401 (2007).
²⁷ E. A. Laird *et al.*, Phys. Rev. Lett. **97**, 056801 (2006).
²⁸ J. R. Petta *et al.*, Phys. Rev. Lett. **100**, 067601 (2008).
²⁹ E. A. Chekhovich *et al.*, Phys. Rev. Lett. **104**, 066804 (2010).
³⁰ R. V. Cherbunin *et al.*, Phys. Rev. B **84**, 041304(R) (2011).
³¹ S. Y. Verbin *et al.*, J. Exp. Theor. Phys **114**, 681 (2012).
³² J. M. Blatt and V. F. Weisskopf, *Theoretical Nuclear Physics*, Springer (1979).
³³ Mandel, L. and Wolf, E. *Optical Coherence and Quantum Optics*, Cambridge (1995).
³⁴ S. Varwig *et al.*, Phys. Rev. B **87**, 115307 (2013).
³⁵ E. A. Chekhovich *et al.*, arXiv:1403.1510 (2014).
³⁶ D. J. Guerrier and R. T. Harley, Appl. Phys. Lett. **70**, 1741 (1997).
³⁷ P. Maletinsky *et al.*, Nat. Phys. **5**, 407 (2009).
³⁸ N. A. Sinitsyn *et al.*, Phys. Rev. Lett. **109**, 166605 (2012).
³⁹ K. Flisinski *et al.*, Phys. Rev. B **82**, 081308(R) (2010).
⁴⁰ C. Bulutay, Phys. Rev. B **85**, 115313 (2012).
⁴¹ M. S. Kuznetsova *et al.*, Phys. Rev. B **89**, 125304 (2014).
⁴² G. Ithier *et al.*, Phys. Rev. B **72**, 134519 (2005).